European Radiology (2019) 29:2740–2750
https://doi.org/10.1007/s00330-018-5878-0

NEURO

Intrauterine fetal MR versus postmortem MR imaging after therapeutic termination of pregnancy: evaluation of the concordance in the detection of brain abnormalities at early gestational stage

Giana Izzo[1] · Giacomo Talenti[2] · Giorgia Falanga[3] · Marco Moscatelli[4] · Giorgio Conte[5] · Elisa Scola[5] · Chiara Doneda[1] · Cecilia Parazzini[1] · Mariangela Rustico[6] · Fabio Triulzi[5] · Andrea Righini[1]

Received: 10 May 2018 / Revised: 16 October 2018 / Accepted: 7 November 2018 / Published online: 12 December 2018

Abstract

Background and purpose Fetal postmortem MR Imaging (pmMRI) has been recently used as an adjuvant tool to conventional brain autopsy after termination of pregnancy (TOP). Our purpose was to compare the diagnostic performance of intrauterine MRI (iuMRI) and pmMRI in the detection of brain anomalies in fetuses at early gestational age (GA).

Material and methods We retrospectively collected 53 fetuses who had undergone iuMRI and pmMRI for suspected brain anomalies. Two pediatric neuroradiologists reviewed iuMRI and pmMRI examinations separately and then together. We used Cohen's *K* to assess the agreement between pmMRI and iuMRI. Using the combined evaluation iuMRI+pMRI as the reference standard, we calculated the "correctness ratio." We used Somers' *D* to assess the cograduation between postmortem image quality and time elapsed after fetus expulsion.

Results Our data showed high agreement between iuMRI and pmMRI considering all the categories together, for both observers (*K*1 0.84; *K*2 0.86). The correctness ratio of iuMRI and pmMRI was 79% and 45% respectively. The major disagreements between iuMRI and pmMRI were related to postmortem changes as the collapse of liquoral structures and distorting phenomena. We also found a significant cograduation between the time elapsed from expulsion and pmMRI contrast resolution and distortive phenomena (both $p < 0.001$).

Conclusions Our study demonstrates an overall high concordance between iuMRI and pmMRI in detecting fetal brain abnormalities at early GA. Nevertheless, for the correct interpretation of pmMRI, the revision of fetal examination seems to be crucial, in particular when time elapsed from expulsion is longer than 24 h.

Key Points

- *IuMRI and pmMRI showed overall high concordance in detecting fetal brain abnormalities at early GA.*
- *PmMRI corroborated the antemortem diagnosis and it could be a valid alternative to conventional brain autopsy, only when the latter cannot be performed.*
- *Some caution should be taken in interpreting pmMR images when performed after 24 h from fetal death.*

Keywords Fetuses · Magnetic resonance imaging · Brain · Termination of pregnancy · Counseling

✉ Giana Izzo
giana.izzo@asst-fbf-sacco.it

[1] Pediatric Radiology and Neuroradiology Department, Children's Hospital V. Buzzi – ASST Fatebenefratelli-Sacco, Via Castelvetro 32, 20154 Milan, Italy

[2] Neuroradiology Unit, Verona University Hospital, Verona, Italy

[3] Department of Neuroradiology, Civico-Di Cristina-Benfratelli Hospital, Palermo, Italy

[4] Postgraduate School in Radiodiagnostics, University of Milan, Milan, Italy

[5] Neuroradiology Unit, Fondazione IRCCS Ca' Granda Ospedale Maggiore Policlinico, Milan, Italy

[6] Obstetrics and Gynecology Department, Children's Hospital V. Buzzi – ASST Fatebenefratelli-Sacco, Milan, Italy

Abbreviations

CNS	Central nervous system
CSF	Cerebrospinal fluid
GA	Gestational age
iuMRI	Intrauterine magnetic resonance imaging
PCF	Posterior cranial fossa
pmMRI	Postmortem magnetic resonance imaging
TOP	Termination of pregnancy

Introduction

Intrauterine fetal imaging techniques, as ultrasound (US) and intrauterine magnetic resonance imaging (iuMRI), represent the current mainstay tool to detect brain abnormalities starting from early gestational age (GA), and their results may impact on decision about possible pregnancy management or termination [1, 2]. However, a definite postmortem diagnosis should be reached in order to provide robust basis for parental counseling about risk of recurrence and to validate the performed obstetric management [3]. Traditionally, brain autopsy has been the reference standard for postmortem diagnosis in fetuses who had undergone termination of pregnancy (TOP) for brain pathologies. However, there has been a steady decline in the rate of brain autopsy over the last years because of various factors (religion objections, ethnic background, emotional factors, and public perceptions) [4, 5]. Moreover, a limitation of conventional brain autopsy is that the fetal brain is predominantly water and once removed from the supporting cerebral spinal fluid (CSF) and skull it collapses, with possible loss of anatomic integrity and deformation [6]; in addiction, it could be affected by maceration-autolysis processes or fixation artifacts may obscure discrete findings [7]. It has been reported that about 20% of brain autopsies are not diagnostic and 10% of them disagree with the antemortem diagnosis [8]. For these reasons, in recent years, less-invasive diagnostic procedures, as postmortem MRI (pmMRI), have emerged as an adjunct and in some cases as an alternative tool to conventional brain autopsy. Recent studies showed that pmMRI can correlate well with cerebral pathological results, with the advantage to examine an intact brain, avoiding the shrinkage and damage of brain tissue occurring during conventional brain autopsy procedures [9, 10]. This technique also offers the opportunity to evaluate the brain "in situ" for lengthy scan time, allowing to obtain high-resolution images (at least four times better than iuMRI imaging) with excellent contrast and signal-to-noise ratio [11] and the potential advantage to better depict some fetal pathological conditions that may be difficult to assess with iuMRI, especially at early GA. For these reasons, in our institution, we started to use pmMRI as an adjunct to conventional brain autopsy to corroborate the antemortem diagnosis; thus, our main purpose was to compare the diagnostic performance between iuMRI and pmMRI in a relevant number of young fetuses (< 24 week of GA), which underwent TOP for suspected brain disorders. We also assessed the influence on image quality of the time elapsed between fetal expulsion and pmMRI examination.

Materials and methods

Fetuses

We retrospectively collected 53 consecutive fetuses below 23 weeks of GA (mean 21.8), who had undergone both iuMRI and pmMRI in our institution between January 2002 and December 2017. All pmMRIs were performed after the TOP for suspected intracranial pathologies at prenatal US or iuMRI, either isolated or part of syndromic conditions. After the TOP, the fetuses were kept in a refrigerator at 4–5 °C prior to the pmMRI.

Unfortunately, only for 21/53 fetuses conventional brain autopsy was performed by board-certified pathologists with special experience in fetal and placental pathology.

Institutional review board approval was obtained.

MR imaging methods

iuMRI examinations were performed on a 1.5 Tesla scanner (Achieva, Philips Medical Systems) using a phased array abdominal coil, with a protocol including multiplanar T2-weighted single-shot fast spin-echo (FSE) sections (TR/TE, 3000/180 ms; voxel size, 1.25 × 1.98 × 3 mm; gap, 0.1 mm; in-plane resolution, 1.02 mm^2), multiplanar balanced steady-state (B-TFE) sections (TR/TE, 7.3/3.7 ms; voxel size 1.47 × 1.46 × 2 mm; gap 0; in-plane resolution 1.05 mm^2), multiplanar T1-weighted FSE sections (TR/TE, 300/14 ms; turbo factor, 3; in-plane resolution, 1.4 mm^2), and, in some cases, axial DWI sections (TR/TE, 1000/90 ms; *b* factor, 0–600 s/mm^2).

pmMRI was performed on both 1.5 and 3.0 Tesla scanners (Achieva, Philips Medical Systems). On 1.5 Tesla scanner, we used the smallest coil the fetus fit in, with a protocol including high-resolution multiplanar T2-weighted FSE sections (TR/TE, 6000/200 ms; voxel size, 0.3 × 0.3 × 2 mm; in-plane resolution 0.26 mm^2; NEX 7), multiplanar T1-weighted SE sections (TR/TE, 406/12 ms; voxel size 0.45 × 0.45 × 2 mm; NEX 5), axial DWI sections (TR/TE, shortest ms; *b* factor, 0–1000 s/mm^2), and sometimes multiplanar BALANCE B-TFE sections (TR/TE, 7/3.5 ms; voxel size 0.59 × 0.59 × 1 mm). On 3 Tesla scanner, the protocol consisted of high-resolution multiplanar T2-weighted FSE sections (TR/TE, 6500/120 ms; voxel size 0.3 × 0.3 × 1.2 mm; NEX 4), sagittal tridimensional T1-weighted fast-field echo sections (TR/TE, 8/4.6 ms; voxel size 0.7 × 0.7 × 0.7 mm; NEX 4), and axial diffusion weighted sections (TR/TE, 2787/60; *b* = 1000; voxel

size 1.6 × 2 × 2 mm). We decided to pool together postmortem cases studied at 1.5 and 3 Tesla (16/53), since the two sets were similar in terms of in-plane resolution.

MR imaging analysis

MR images were analyzed by two pediatric neuroradiologists with 3 years of experience in fetal imaging, according to predefined categories, divided by the basis of location (i.e., midline structure anomalies) and pathophysiological mechanism (malformative or lesional) and subcategories by the type of pathology (i.e., callosal agenesis in the group of midline structure anomalies), as shown in Table 1. The two observers firstly evaluated each pmMRI separately (first reading session) and blinded to the results of the corresponding iuMRI and after a few weeks they evaluated iuMRIs (second reading session). Then, pmMRI+iuMRI were reviewed together (third reading session), since the approach of comparing together the findings between the iuMRI and pmMRI of the same fetus reflects the ordinary practice in clinical setting. Image quality of pmMRI was assessed in terms of image contrast resolution on T2-weighted images (3 good, 2 acceptable, 1 poor), considering signal homogeneity and visualization of the brain layers characteristic of fetal brain development [12] and distortive phenomena (3 severe, 2 mild, 1 none). The visual assessment of the two different pools of images (1.5 T and 3 T) was judged to be not substantially different in terms of signal contrast between structures.

Statistical analysis

We evaluated the interobserver agreement (reader 1 vs reader 2) considering all categories together with Cohen's kappa for each reading session (iuMRI, pmMRI, and iuMRI+pmMRI). Considering the almost-perfect interobserver agreement (see the "Results" section), we evaluated the intersession agreement (iuMRI vs pmMRI, iuMRI vs iuMRI+pmMRI, pmMRI vs iuMRI+pmMRI) with Cohen's kappa only for the reader 1, as well as in the further statistical analysis. For this analysis, each finding (in categories as well as in subcategories) was considered nominal variable (absent/present). Since more than one finding was sometimes observed in a single fetus (subject), we chose to consider each finding a case, so we had more cases than subjects (fetuses). As we could not use the conventional brain autopsy as the reference standard, we considered the iuMRI+pmMRI session the reference standard and we defined iuMRI and pmMRI "correctness ratio" as the percentage of the iuMRI and the pmMRI correct examinations (subjects/fetuses). A further analysis aimed to analyze the non-correct iuMRI examinations in order to answer to the question "did pmMRI change the main diagnosis and influence the parental counselling?" (yes or no). We used Somers' *D* to assess the relation of the pmMRI contrast resolution quality and distortive phenomena with the time elapsed between the fetus expulsion and the MR examination (less than 24 h, between 24 and 48 h, more than 48 h). We considered the time of fetus expulsion the time of fetus demise because the TOP in our institution is performed before 23 weeks of gestation without intrauterine administration of feticide substances. Statistical analysis was performed using the SPSS 21.0 for Windows software package (SPSS Inc.).

Results

Interobserver agreement

Observer 1 At the iuMRI session, a total of 148 findings were reported. At the pmMRI session, a total of 144 findings were reported. At the iuMRI+pmMRI session, a total of 156 findings were reported.

Observer 2 At the iuMRI session, a total of 155 findings were reported. At the pmMRI session, a total of 158 findings were reported. At the iuMRI+pmMRI session, a total of 167 findings were reported.

The overall interobserver agreement for iuMRI session was $K = 0.83$ (std. error 0.03); for pmMRI session, $K = 0.82$ (std. error 0.03); and for the iuMRI+pmMRI session, $K = 0.82$ (std. error 0.03).

Intersession agreement

The results are listed in Table 1.

Correctness ratio

Using the iuMRI+pmMRI session as the reference standard, the "correctness ratio" of iuMRI was 79% (42/53 examinations correctly evaluated) and for pmMRI was 45% (24/53 examinations correctly evaluated). In particular, at the iuMRI session, among the 11 examinations evaluated as incorrect in relation to discordant findings with the reference standard, 3/11 were considered pathologic ("false positive": 1 examination with corpus callosum agenesis, 1 with ischemic lesion, 1 with hemorrhagic lesion), while 8/11 were reported as "normal" ("false negative": 1 examination with hypothalamic thickening, 1 with cerebellar dysplasia, 1 with polymicrogyria, 1 with hemorrhagic lesion, 4 with layers anomalies). At the pmMRI session, among the 29 examinations evaluated as incorrect in relation to discordant findings with the reference standard, 6/29 were considered pathologic ("false positive": 2 with hypothalamic region thickening, 1 with brainstem dysmorphism, 1 with layer anomaly, 1 with ventricular dysmorphism, 1 with cisterna magna widening) while 23/29 were reported as "normal" ("false negative": 2 with corpus callosum dysmorphism, 3 with microcephaly, 2

Table 1 MR findings divided into categories and subcategories are listed; the diagnostic performance of iuMRI session and pmMRI session and the results from the joint evaluation of both techniques (iuMRI+pmMRI) are reported for each category. In the last three columns, the intersession agreement (iuMRI vs pmMRI, iuMRI vs iuMRI+pmMRI, pmMRI vs iuMRI+pmMRI) is reported

Categories Subcategories	iuMRI	pmMRI	iuMRI+pmMRI	iuMRI vs pmMRI *K*	iuMRI vs iuMRI+pmMRI *K*	pmMRI vs iuMRI+pmMRI *K*
Midline				0.82	0.94	0.88
Corpus callosum agenesis	8	7	7			
Corpus callosum dysmorphism	10	10	10			
Corpus callosum thinning	15	15	15			
Septum pellucidum agenesis	3	3	3			
Hypothalamic region thickening	*0*	*3*	*1*			
Holoprosencephaly	2	2	2			
Total	38	40	38			
PCF				0.91	0.94	0.89
Rhombencephalosynapsis	3	3	3			
Molar tooth malformation	2	2	2			
Giant tectum	2	2	2			
Aqueductal stenosis	10	10	10			
Ponto-cerebellar hypoplasia	2	2	2			
Cerebellar vermis hypoplasia	13	13	13			
Cerebellar vermis rotation	*10*	*7*	*10*			
Cerebellar agenesis	1	1	1			
Cerebellar dysplasia	1	2	2			
Chiari II malformation	1	1	1			
Brain stem dysmorphism	14	15	14			
Pontine tegmental cap	1	1	1			
Total	60	59	61			
Corticals				0.64	0.96	0.68
Microcephaly	*8*	*5*	*8*			
Macrocephaly	*2*	*0*	*2*			
Hemimegalencephaly	1	1	1			
Lissencephaly	2	2	2			
Gray matter heterotopias	1	1	1			
Polymicrogyria	9	9	10			
Schizencephaly	1	1	1			
Opercular anomalies	*5*	*3*	*5*			
Total	29	22	30			
CSF structures				0.65	1	0.65
Ventriculomegaly	21	18	21			
Ventricular dysmorphism	32	32	32			
Cisterna magna widening	6	3	6			
Supratentorial liquoral spaces widening	*22*	*8*	*22*			
Arachnoid cysts	3	3	3			
Myelomeningocele	1	1	1			
Total	*85*	*65*	*85*			
Acquired				0.36	0.5	0.83
Ischemic alterations	*3*	*2*	*2*			
Hemorrhagic alterations	*2*	*3*	3			
Infective alterations	2	2	2			

Table 1 (continued)

Categories						
Subcategories	iuMRI	pmMRI	iuMRI+pmMRI	iuMRI vs pmMRI *K*	iuMRI vs iuMRI+pmMRI *K*	pmMRI vs iuMRI+pmMRI *K*
Total	7	7	7			
Others				0.75	0.69	0.93
Basal ganglia dysmorphism	4	4	4			
Diencephalic-mesencephalic junction dysplasia	4	4	4			
Ganglionic eminence hypertrophism	1	1	1			
Ganglionic eminence cavitations	2	2	2			
Layers anomalies	*5*	*9*	*9*			
Total	16	20	20			

Italics numbers represent the major discrepancies between iuMRI and pmMRI among the different subcategories, as reported in the discussion session

with macrocephaly, 1 with polymicrogyria, 2 with opercular anomalies, 3 with cerebellar vermis rotation, 3 with mild ventriculomegaly, 1 with ventricular dysmorphism, 14 with supratentorial liquoral space widening, 3 with cisterna magna widening) (some examinations had more than one finding). The subcategory "ventricular dysmorphism" referred to the abnormal shape of lateral ventricles that can result from different conditions such as midline abnormalities, most frequently regarding corpus callosum (agenesis/dysgenesis) or septum pellucidum, and genetic conditions (in these cases, the morphology of frontal horns may tend to be square shaped). Also, "hypothalamic thickening" referred to appearance of hypothalamus-infundibular region when a hamartoma of the tuber cinereum occurs.

In 2/11 cases in which iuMRI was considered incorrect, pmMRI changed the main diagnosis and influenced the parental counseling.

Cograduation for image quality for postmortem evaluation

We found a significant cograduation between the time elapsed from the expulsion and the pmMRI (independent) and the two variables of image quality (dependent): namely a negative cograduation for contrast resolution (Somers' D −0.44, $p < 0.001$) and a positive cograduation for distortive phenomena (Somers' D 0.60, $p < 0.001$), as the graphic shows (Fig. 1).

Conventional brain autopsy studies, when available (21/53 cases), confirmed all the results reported by the iuMRI+pmMRI session.

Discussion

In our study, we found an overall good agreement between iuMRI and pmMRI in the detection of intracranial pathologies in fetuses at early GA (< 24 week), considering either all categories together or each single category. The concordance was higher for midline (Fig. 2) and posterior cranial fossa (PCF) malformations (Fig. 3) (K = near perfect) than for cortical malformations, CSF structure anomalies, and "other anomalies" group (K = substantial), while it was only fair for acquired (clastic) lesions. Our results strengthened the results of the only similar work regarding a 12 early fetuses cohort (25 mean GA) where brain findings of the in utero imaging (US and MRI) were compared with those of postmortem examinations (pmMRI plus traditional conventional brain autopsy) and iuMR imaging provided a correct diagnosis in all the cases [13]. Thus, our observation supports what was recently reported by the multicentric MERIDIAN study (total fetuses

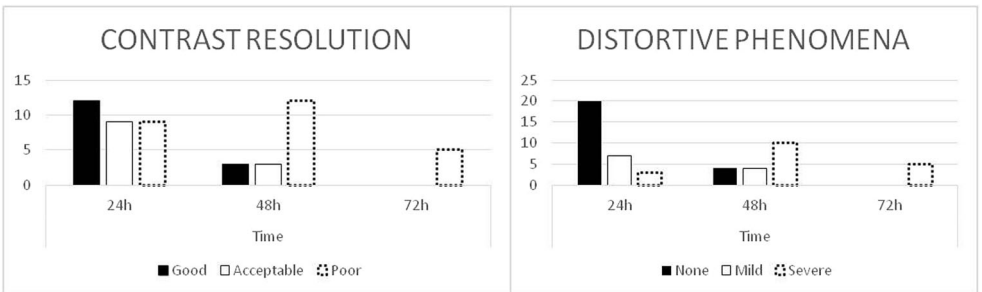

Fig. 1 Contrast resolution and distortive phenomena plotted against time elapsed from fetus expulsion. On the ordinate axis the count of cases grouped by categories of the outcome variable

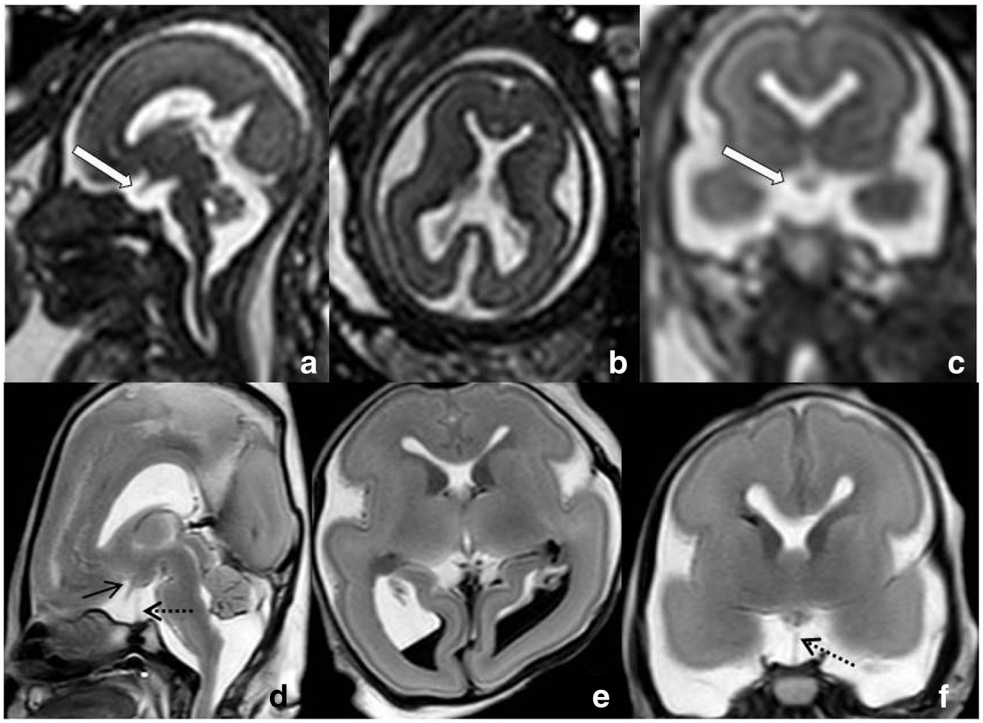

Fig. 2 (**a**–**c**) Fetal multiplanar BALANCE B-TFE images show the agenesis of septum pellucidum, giving the typical squared shape of the frontal horns (**b**, **c**). The optic chiasm is well depicted (white arrows in **a**, **c**) while the pituitary stalk is less clearly appreciable. (**d**–**f**) Postmortem multiplanar FSE high-resolution T2-weighted images show the agenesis of septum pellucidum (**e**, **f**) and better demonstrate the presence of pituitary stalk (dashed black arrows in **d**, **f**). In **d**, thickening of hypothalamic region is also noted (black arrow) interpreted as a possible hypothalamic hamartoma, but not confirmed after reviewing iuMRI

570; 369 < 24 GA) concerning the high overall diagnostic accuracy (93%) of iuMRI at early fetal stage [14]. To date, pmMRI accuracy has been compared only with the results of conventional brain autopsy. A large sub-analysis by MARIAS group reported an overall good diagnostic accuracy of pmMRI in fetuses < 24 week GA, with a sensibility and specificity of 87% and 69% respectively and a concordance with conventional brain autopsy of 73% [15]; similar results were reported in 40 fetuses (14–40 week GA) by Griffiths et al (sensitivity 100%, specificity 92%, PPV 95%, NPV 100%,

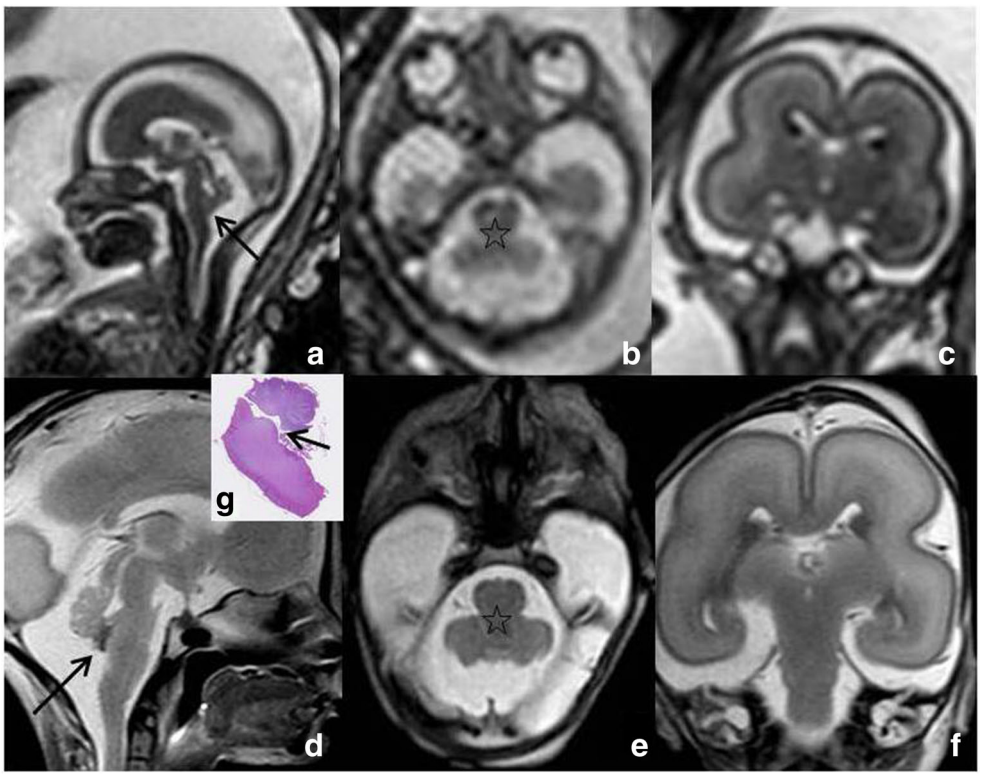

Fig. 3 **a**–**c** Fetal multiplanar BALANCE B-TFE sequences demonstrate a dysmorphic brainstem due to reduction in size of the pons, with almost absent pontine bulging (**a**, **b**). The cerebellar structures are also small. Posteriorly to the pons, a reverse bulging is appreciable just at the junction with the medulla oblongata (black arrow in **a** and little star in **b**), as "tegmental cap" sign. **d**–**f** Postmortem multiplanar FSE high-resolution T2-weighted images depict all the prenatal findings with hemosiderin deposits/choroid plexus just adjacent to the tegmental cap (black arrow in **d** and little star in **e**). In **f**, also note the associated agenesis of internal auditory canals, not clearly evident on fetal images. The pathological specimen (**g**) demonstrates the tegmental cap (arrow)

with an agreement with conventional brain autopsy of up to 97%) [16]. Furthermore, few studies suggested the superiority of pmMRI over conventional brain autopsy for visualization of neuroanatomy and neurological anomalies, in particular for FCP anomalies and ventriculomegaly [17, 18]. Nevertheless in the present study the correctness ratio of iuMRI was actually higher than that of pmMRI (79% vs 45%), with 42/53 and 24/53 examinations respectively correctly identified; however for this kind of analysis we considered each examination a case, instead for the analysis of the interobserver and intersession agreement we considered each single finding a case. Anyway when the findings of iuMRI and pmMRI were reviewed together (iuMR+pmMR session) we found an increased agreement for all the categories; in particular, the concordance rose up in most of categories (cortical malformations, CSF structures anomalies, midline and PCF malformations) after a re-evaluation of prenatal findings compared to ones of the pmMRI. Meanwhile, we found the opposite result in the categories "other anomalies" and "acquired lesions". The major differences that we observed between iuMRI and pmMRI concerned the category "CSF structures anomalies" and in particular the subarachnoid spaces (Fig. 4). This result markedly reduced the "correctness ratio" of pmMRI (23/29 examinations that were incorrectly evaluated at pmMRI session with respect to the reference standard regarded CSF structures anomalies as discordant findings). These discrepancies were due to the reduction in size of CSF structures in the postmortem brain, presumably because of the loss of CSF pressure. This phenomenon was previously observed by Sebire et al, who reported the frequent resolution of fetal ventriculomegaly after death at pmMRI and conventional brain autopsy [19]. In our study as well, three cases of mild ventriculomegaly (atrium 10–12 mm) were missed by pmMRI, whereas conditions of severe ventriculomegaly (atrium > 15–16 mm) were all identified. We also noted that the decrease in size of CSF structures correlated with the time elapsed from the fetus expulsion, suggesting that this phenomenon could be due also to a combination of multiple effects following death, as CSF shift and changes in the mechanical characteristics of brain structures. Likewise, in the category "midline malformations," pmMRI found two alterations regarding the hypothalamic region, not observed at iuMRI and not confirmed after reviewing both results in consensus (Fig. 2); this could be due to the postmortem mechanical distorting phenomena with drooping of the hypothalamus toward the anterior recesses of the third ventricle, determining a thick aspect of this portion and misinterpreted as a hypothalamic hamartoma. On the same line, also in the category "PCF malformations," pmMRI missed three cases of cerebellar vermis upward rotation, confirmed by the review of iuMRI findings and associated to vermis hypoplasia (this latter accurately identified by pmMRI); in one case as well, brainstem dysmorphism was incorrectly assessed by pmMRI probably due to postmortem distortion. On the contrary, pmMRI

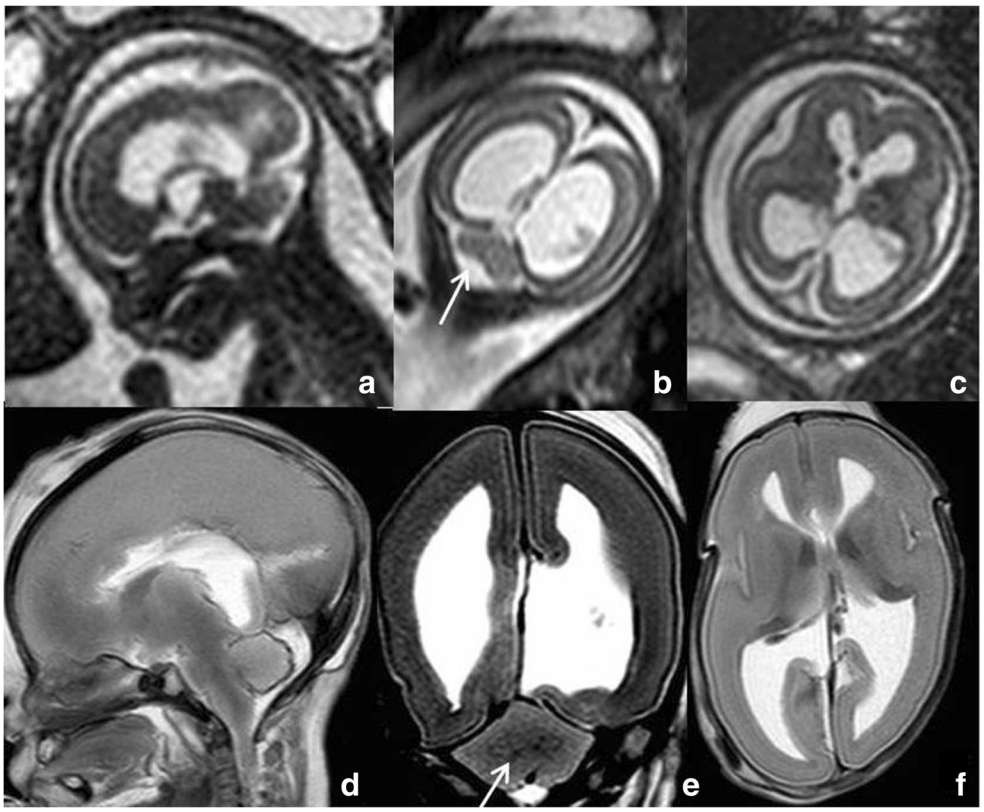

Fig. 4 (**a**–**c**) Fetal multiplanar BALANCE B-TFE sequences show severe ventriculomegaly secondary to aqueductal stenosis in a case of rhombencephalosynapsis (white arrow in **b**). Subarachnoid spaces are reduced in size but still appreciable. **d**–**f** Postmortem multiplanar FSE high-resolution T2-weighted images demonstrate the ventriculomegaly as well, even if less pronounced with respect to what is evident on fetal MRI, and the liquoral spaces are diffusely obliterated. Postmortem distortion of cerebral structures and maceration phenomena with cancelation of parenchymal layers are also evident, since the study was performed more than 24 h after fetal expulsion. Note how the cerebellar hemisphere fusion is more evident on pmMRI with respect to iuMRI, also showing the fusion of dentate nuclei (white arrow in **e**)

reported one case of cerebellar dysplasia not observed prenatally and then confirmed by the revaluation of both iuMRI and pmMRI together. This discrepancy could be addressed by the small volume of the cerebellum at early GA leading to a more difficult assessment of the foliation by iuMRI than by pmMRI [20]. Even if we expected a better performance of pmMRI in the category of "cortical malformations," iuMRI identified three cases of moderate microcephaly and two cases of macrocephaly not identified by pmMRI. This disagreement could be due to the more accurate estimation of brain and cranial volume by iuMRI in particular in cases of increased cranial size and CSF spaces; instead, at pmMRI, the brain parenchyma and CSF space distortion could make difficult the assessment of brain volume. Despite that we previously reported the relatively low sensitivity of iuMRI (64.7%) in the detection of disorders of cortical development as polymicrogyria and heterotopias [21], of 10 cases of polymicrogyria confirmed at the iuMR+pmMR session, only one case of anomalous temporal-basal sulcation was missed prenatally. On the contrary, one case of anomalous sulcus was detected only by iuMRI, though the quality of pmMRI images in such case was poor because of postmortem destructive phenomena.

On the other hand, for the category "acquired lesions," the concordance between the two techniques increased when the MRI findings were reviewed with the support of pmMRI, even if the results were statistically affected by the small number of observations in this class. For example, in the case of cerebellar vermis slightly reduced in size and upward rotated with associated ventriculomegaly, pmMRI detected the presence of large amount of hemosiderin deposits within ventricles and cisterna magna, diversely from the typical intraventricular small clots of postmortem bleedings, so it was correctly addressed to a result of intrauterine intraventricular hemorrhage (Fig. 5); conversely, at iuMRI, the examination was interpreted as a PCF malformation. In a case of microcephaly with diffuse irregularity of the cortical surface and apparent parenchymal signal alterations at iuMRI, therefore classified in the group of ischemic lesions, at the iuMRI+pmMRI session, the condition was interpreted as probable genetic microcephaly on the basis of pmMRI findings; in this case, the brain mantle, even if thinner than normal, resulted intact without any focal signal alteration. These are the only two cases where iuMRI was evaluated as incorrect with respect to the reference standard and where pmMRI changed the main diagnosis with significant impact on the parental counseling, allowing to establish the genetic risk of recurrence in the second case. The other two hemorrhagic lesions were distinguishable from postmortem bleeds at pmMRI by their intraparenchymal location, along the deep medullary vein territory in one case and within the cerebellar hemispheres in the other one. The two infectious processes (cytomegalovirus) were correctly suspected on the basis of periventricular calcifications, destructive lesions in the basal ganglia and cortex with cortical irregularity, and parenchymal thinning in microcephalic fetuses. The analysis of placental CMV-PCR and fetal serology confirmed our hypothesis. The sub-analysis made by MARIAS group [15] reported pmMRI sensitivity for intracranial bleeds of 100% and a poor sensitivity and PPV (30%) for antemortem ischemic lesion compared to conventional brain autopsy. They addressed these results to some postmortem changes related to autolysis and maceration phenomena: the loss of gray-white matter differentiation, the loss of the normal high signal in the posterior limb of internal capsule, and white matter T2 value prolongation [22, 23]. However, T1 and T2 signal changes were mostly described in fixed brain due to excess of tissue dehydration and cooling [24]; we did not note such signal modifications in the majority of postmortem images, probably because we studied fresh and unfixed fetal brains. Nevertheless, tissue contrast tended to reduce progressively over time: in cases of pmMRI performed after more than 24 h from expulsion, the T2-weighted tissue contrast was clearly reduced and it was poor after 48 h (Fig. 1). Timing also affected the neuroanatomy because of distortion and shrinking of brain structures (Fig. 1). PmMRI showed four cases of layer alterations (in the category "others") not detected by iuMRI; these were mostly cases with microlissencephaly and derangement of cerebral lamination (Fig. 6); in this cases, the higher spatial and contrast resolution of pmMRI better depicted the transient parenchymal layers of the second trimester, representing a landmark of fetal brain development [25, 26]. At the current in-plane spatial resolution of iuMRI (about 1 mm^2), very few pixels can fit within each different layer (i.e., periventricular zone, intermediate zone, subplate, cortical plate); meanwhile, pmMRI can take advantage of a spatial resolution which is at least four times better, so to ease the distinction between the different layers. It is likely that some limitation of iuMRI in detecting brain mantle layering abnormalities could be at least partially overcome in the near future by using higher resolution imaging on new-generation 3 Tesla scanners. Abnormal laminar organization of the fetal cerebrum has been previously described on postmortem T1- and T2-weighted MRI in a single case of lissencephaly cobblestone complex, matching with histopathology [27]. An original research reported an overall sensitivity and NPV of T1-weighted images higher than the ones obtained by T2-weighted in assessing the cerebral lamination, which instead had a higher specificity and PPV [28]. In our cases, only T2-weighed high-resolution images were considered able to nicely depict the cerebral layers, because tissue contrast on T1-weighted images was poor in unfixed brains.

Study limitations

The major limitations of our work are the following: (1) we used as the reference standard the combined evaluation of

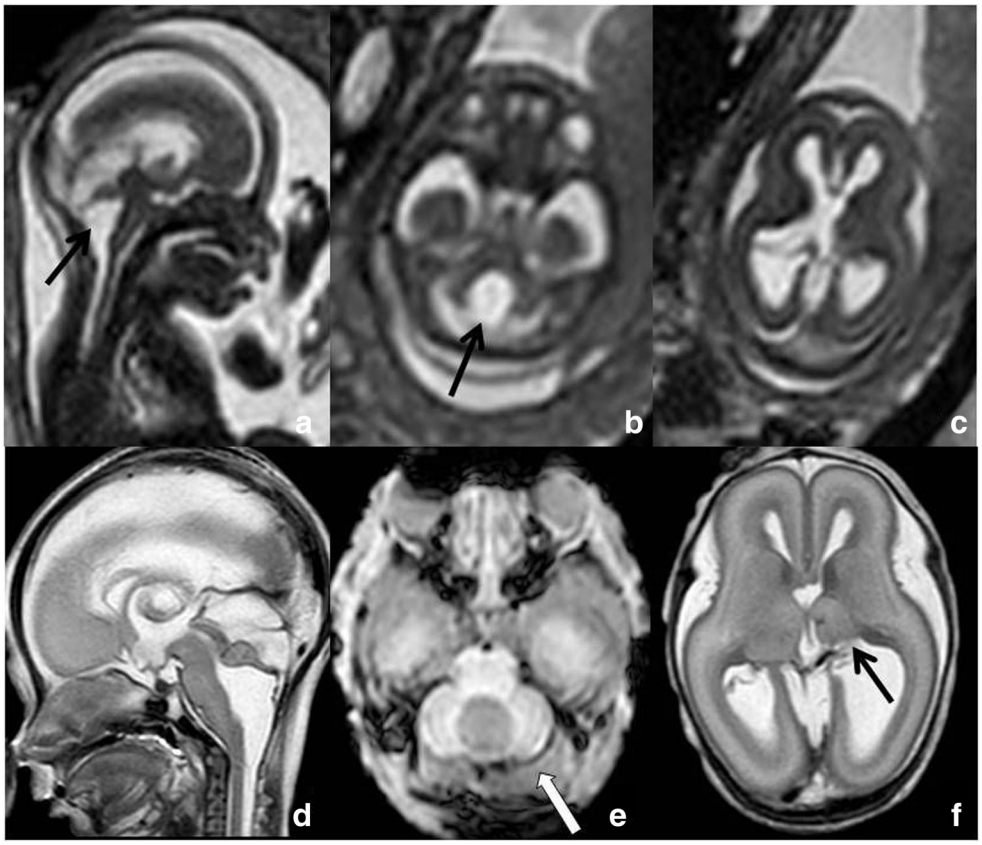

Fig. 5 **a–c** Fetal multiplanar BALANCE B-TFE sequences show reduction of cerebellar structures with upward counterclockwise rotation of the vermis and consequent widening of the inferior aspect of the IV ventricle and cisterna magna (black arrows in **a**, **b**). A mild ventriculomegaly is also evident (**c**); the Sylvian aqueduct is not clearly visible (**a**). Based on these images, the diagnosis of PCF malformation was made. **d–f** In the same fetus, pmMRI axial susceptibility weighted image (**e**) nicely depicts hemosiderin deposits in the cisterna magna (white arrow); these findings raise the hypothesis of intraventricular bleeding with possible obliteration of the IV ventricle outlet foramina and consequent tetra ventricular dilatation, as shown on sagittal and axial FSE high-resolution T2-weighted images (**d**, **f**). In this case, the upward rotation of the cerebellar vermis is preserved and it may be related to the presence of post-hemorrhagic adhesions (**d**). In **f**, also note the hemorrhagic lesion of one thalamus with volume loss, as the consequence of the same insult (black arrow)

iuMRI and pmMRI instead of conventional brain autopsy, that it is still considered the gold standard for postmortem evaluation [29, 30]. While it is reasonable to state that macroscopic and coarse anomalies are likely to be substantially characterized by pmMRI, the microscopic examination of the tissue and the immunohistochemical sampling are fundamental to refine the macroscopic diagnosis and to ease possible correlation with advanced genetic testing. Unfortunately, only for 21 fetuses conventional brain autopsy results were available, so they could not be used as a gold standard in our study. This observation reflects the critical situation present in many countries and underlines the practical concern that led us to undertake this study. Although there is large variation in different nations and communities, the rate of performing fetal conventional brain autopsy is low in many countries and hence some women are without valuable information about the risk in future pregnancies. The reason for this is complicated, but legal frameworks that do not mandate conventional brain autopsy and religious beliefs that require rapid funeral arrangements are central to the discussion. This paper, therefore, takes the view that, although conventional brain autopsy should be offered, families that decide not to accept that can benefit from an imaging-based non-invasive alternative to receive "as good information as possible" in these circumstances. There is good evidence now that the results of pmMR for the fetal brain closely match conventional brain autopsy [15, 16, 18] and good-quality evidence that iuMR has a diagnostic accuracy of approximately 95% (MERIDIAN study) [14]. On this basis, we believe that the pragmatic approach of using a combined reading of iuMR and pmMR imaging provides a reliable "reference" standard even if it is not a "gold" standard.

The second main limitation was that iuMRI and pmMRI were all related to abnormal examinations. For these reasons, we could not evaluate diagnostic accuracy because of the lack of negative examinations.

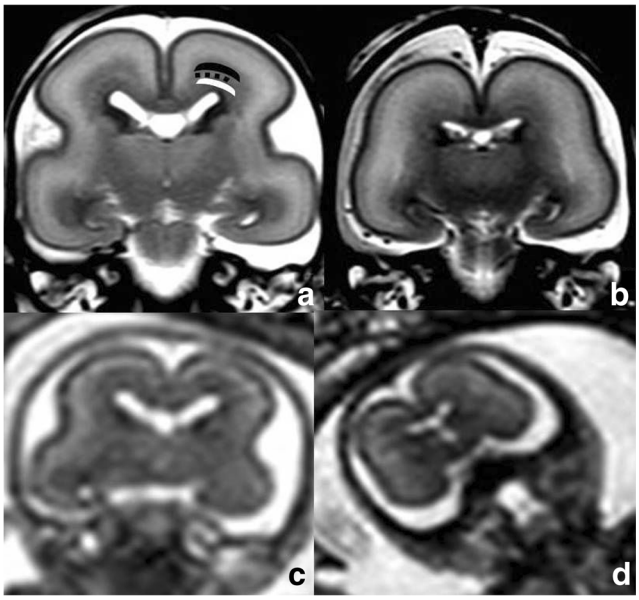

Fig. 6 **a–b** Postmortem coronal FSE high-resolution T2-weighted images show the comparison between the normal pattern of transient fetal cerebral lamination (**a**) and the abnormal one (**b**) in a case of microlissencephaly. In **a**, note the normal intermediate zone (black arch), separated from the germinal matrix (white arch) by a thin layer (dashed black arch) corresponding to subventricular zone; the intermediate zone is also well delineated from the thick subplate above. On the contrary, in **b**, the intermediate zone results thicker without a clear separation from the germinal matrix and the subplate. **c–d** On fetal coronal BALANCE B-TFE images (**c**, **d**) even if some parenchymal layers are visible, the cerebral lamination is not as clearly defined as being abnormal in **d**

Conclusion

Our study demonstrated the overall high concordance between iuMRI and pmMRI in detecting fetal brain abnormalities at early gestational age. We also confirmed the diagnostic value of iuMRI in prenatal diagnosis and obstetric management providing important information for parental counseling. Despite the technical advantages of pmMRI, its correctness ratio is fairly lower; so for the correct interpretation of pmMR imaging, a close match with iuMRI seems to be crucial. As for conventional brain autopsy, the major limits are represented by the postmortem phenomena; in particular, the reduction in size and deformation of CSF structures could masque some pathologic conditions, as microcephaly or some aspects of posterior cranial fossa malformations.

Acknowledgments We are grateful to Professor Paul D. Griffiths for his advice in preparing the manuscript.

Funding The authors state that this work has not received any funding.

Compliance with ethical standards

Guarantor The scientific guarantor of this publication is Andrea Righini, chief of the Neuroradiology Department.

Conflict of interest The authors of this manuscript declare no relationships with any companies, whose products or services may be related to the subject matter of the article.

Statistics and biometry No complex statistical methods were necessary for this paper. One of the authors has statistical expertise.

Informed consent Written informed consent was obtained from all subjects in this study.

Ethical approval Institutional review board approval was obtained.

Study subjects or cohorts overlap One study case has been previously reported in *Prenatal Magnetic Resonance Imaging of Atypical Partial Rhombencephalosynapsis with involvement of the Anterior Vermis: Two Case Reports.* Izzo G, Conte G, Cesaretti C, Parazzini C, Bulfamante G, Righini A. Neuropediatrics. 2015 Dec;46(6):416–9.

Methodology
- retrospective
- diagnostic or prognostic study
- performed at one institution

References

1. Glenn OA (2006) Fetal central nervous system MR imaging. Neuroimaging Clin N Am 16(1):1–17
2. Jarvis D, Mooney C, Cohen J et al (2017) A systematic review and meta-analysis to determine the contribution of mr imaging to the diagnosis of foetal brain abnormalities in utero. Eur Radiol 27(6): 2367–2380
3. Huisman TA, Wisser J, Stallmach T, Krestin GP, Huch R, Kubik-Huch RA (2002) MR conventional brain autopsy in fetuses. Fetal Diagn Ther 17:58–64
4. Griffiths PD, Paley MN, Whitby EH (2005) Post-mortem MRI as an adjunct to fetal or neonatal conventional brain autopsy. Lancet 365:1271–1273
5. Addison S, Arthurs OJ, Thayyil S (2014) Post-mortem MRI as an alternative to non forensic conventional brain autopsy in fetuses and children: from research into clinical practice. Br J Radiol. https://doi.org/10.1259/bjr.20130621
6. Brookes JS, Hagmann C (2006) MRI in fetal necroscopy. J Magn Reson Imaging 24:1221–1228
7. Pfefferbaum A, Sullivan EV, Adalsteinsson E, Garrick T, Harper C (2004) Postmortem MR imaging of formalin-fixed human brain. Neuroimage 21:1585–1595
8. Thayyil S, Sebire NJ, Chitty LS et al (2011) Post mortem magnetic resonance imaging in the fetuses, infant and child : a comparative study with conventional conventional brain autopsy (MaRIAS protocol). BMC Pediatr. https://doi.org/10.1186/1471-2431-11-120
9. Lequin MH, Huisman TA (2012) Postmortem MR imaging in the fetal and neonatal period. Magn Reson Imaging Clin N Am 20: 129–143
10. Whitby EH, Paley MN, Cohen M, Griffiths PD (2005) Postmortem MR imaging of the fetus: an adjunct or a replacement for conventional conventional brain autopsy? Semin Fetal Neonatal Med 10: 475–483
11. Breeze AC, Cross JJ, Hackett GA et al (2006) Use of a confidence scale in reporting postmortem fetal magnetic resonance imaging. Ultrasound Obstet Gynecol 28:918–924
12. Scola E, Conte G, Palumbo G et al (2018) High resolution postmortem MRI of non fixed in situ foetal brain in the second trimester

of gestation : normal foetal brain development. Eur Radiol 28(1): 363–371
13. Whitby EH, Variend S, Rutter S et al (2004) Corroboration of in utero MRI using post-mortem MRI and conventional brain autopsy in foetuses with CNS abnormalities. Clin Radiol 59:1114–1120
14. Griffiths PD, Bradburn M, Campbell MJ et al (2017) Use of MRI in the diagnosis of fetal brain abnormalities in utero (MERIDIAN): a multicentre, prospective cohort study. Lancet 389(10068):538–546
15. Arthurs OJ, Thayyil S, Pauliah SS et al (2015) Diagnostic accuracy and limitations of post-mortem MRI for neurological abnormalities in fetuses and children. Clin Radiol 70:872–800
16. Griffiths PD, Varient D, Evans M et al (2003) Postmortem MR imaging of the fetal and stillborn central nervous system. AJNR Am J Neuroradiol 24:22–27
17. Whitby EH, Paley MN, Cohen M, Griffiths PD (2006) Post-mortem fetal MRI: what do we learn from it? Eur J Radiol 57:250–255
18. Thayyil S, Sebire N, Chitty LS et al (2013) Post-mortem MRI versus conventional conventional brain autopsy in fetuses and children: a prospective validation study. Lancet 382:223–233
19. Sebire NJ, Miller S, Jacques TS et al (2013) Post-mortem apparent resolution of fetal ventriculomegaly : evidence from magnetic resonance imaging. Prenat Diagn 33:360–364
20. Garel C, Fallet-Bianco C, Guibaud L (2011) The fetal cerebellum: development and common malformations. J Child Neurol 26(12): 1483–1492
21. Conte G, Parazzini C, Falanga G et al (2016) Diagnostic value of prenatal MR imaging in the detection of brain malformations in fetuses before the 26th week of gestational age. AJNR 37(5):946–951
22. Thayyil S, De Vita E, Sebire NJ et al (2012) Post-mortem cerebral magnetic resonance imaging T1 and T2 in fetuses, newborns and infants. Eur J Radiol 81:232–238
23. Montaldo P, Addison S, Oliveira V et al (2016) Quantification of maceration changes using post mortem MRI in fetuses. BMC Med Imaging. https://doi.org/10.1186/s12880-016-0137-9
24. Verhoye M, Votino C, Cannie MM et al (2013) Post-mortem high-field magnetic resonance imaging: effect of various factors. J Matern Fetal Neonatal Med 26(11):1060–1065
25. Kostovic I, Judas M, Rados M, Hrabac P (2002) Laminar organization of the human fetal cerebrum revealed by histochemical markers and magnetic resonance imaging. Cereb Cortex 12:536–544
26. Zhang Z, Liu S, Lin X et al (2011) Development of fetal brain of 20 weeks gestational age: assessment with post-mortem magnetic resonance imaging. Eur J Radiol 80(3):e432–e439
27. Widjaja E, Geibprasert S, Blaser S, Rayner T, Shannon P (2009) Abnormal fetal cerebral lamination in cobbleston complex seen on post-mortem MRI and DTI. Pediatr Radiol 38:860–864
28. Widjaja E, Geibprasert S, Mahmoodabadi SZ, Brown NE, Shannon P (2010) Corroboration of normal and abnormal fetal cerebral lamination on post mortem MR imaging with postmortem examination. AJNR 31:1987–1993
29. Sebire NJ (2006) Towards the minimally invasive conventional brain autopsy? Ultrasound Obstet Gynecol 28:865–867
30. Breeze AC, Jessop FA, Set PA et al (2011) Minimally-invasive fetal autopsy using magnetic resonance imaging and percutaneus organ biopsies: clinical value and comparison to conventional autopsy. Ultrasound Obstet Gynecol 37:317–323